Molecular Crystals and Liquid Crystals Science and Technology. Section A. Molecular Crystals and Liquid Crystals

Publication details, including instructions for authors and subscription information:
http://www.tandfonline.com/loi/gmcl19

Cage Effects in the Orientational Dynamics of a Gay-Berne Mesogen

Giacomo Saielli [a], Antonino Polimeno [a], Pier Luigi Nordio [a], Martin A. Bates [b] & Geoffrey R. Luckhurst [b]

[a] Dipartimento di Chimica Fisica Università di Padova, Via Loredan 2, 35131, Padova, ITALY

[b] Department of Chemistry and Southampton Liquid Crystal Institute, University of Southampton, Highfield, Southampton, SO17 1BJ, UK

Version of record first published: 24 Sep 2006

To cite this article: Giacomo Saielli, Antonino Polimeno, Pier Luigi Nordio, Martin A. Bates & Geoffrey R. Luckhurst (1999): Cage Effects in the Orientational Dynamics of a Gay-Berne Mesogen, Molecular Crystals and Liquid Crystals Science and Technology. Section A. Molecular Crystals and Liquid Crystals, 336:1, 47-59

To link to this article: http://dx.doi.org/10.1080/10587259908026020

Mol. Cryst. and Liq. Cryst., 1999, Vol. 336, pp. 47-59
Reprints available directly from the publisher
Photocopying permitted by license only

Cage Effects in the Orientational Dynamics of a Gay-Berne Mesogen

GIACOMO SAIELLI[a], ANTONINO POLIMENO[a*], PIER LUIGI NORDIO[†], MARTIN A. BATES[b] and GEOFFREY R. LUCKHURST[b]

[a]*Dipartimento di Chimica Fisica Università di Padova, Via Loredan 2, 35131 Padova, ITALY and* [b]*Department of Chemistry and Southampton Liquid Crystal Institute, University of Southampton, Highfield, Southampton SO17 1BJ, UK*

The dynamical features of a Gay-Berne mesogen have been investigated through an analysis of molecular dynamics simulation data. The cage potential confining instantaneously the orientational motion of the molecules, for both the isotropic and nematic phases have been defined and parameterised. The statistical analysis of the data obtained from the MD simulations show that no significant differences exist in the local structural and dynamical properties of the cage in the isotropic and nematic phases, but that a clear dependence of the cage potential does exist with respect to its orientation in the nematic phase.

Keywords: cage; orientational dynamics; Gay-Berne mesogen; liquid crystal

INTRODUCTION

The orientational dynamics of a molecule in a dense fluid are still far from being completely understood. Several dynamical processes take place, which govern the molecular reorientational motion on different timescales. The situation is even more complex in a partially ordered phase, like a nematic

* Corresponding author
† Deceased

liquid crystal, where the effect of the anisotropic environment has to be taken into account.

In a very simplified view we can state that in a liquid phase, both isotropic and nematic, two distinct dynamical regimes can be identified: a slow diffusive regime ($10^2 \div 10^3$ ps) and a much faster inertial regime ($\leq$ 1 ps). Evidence of the latter process comes both from computer simulations as well as experiments. Molecular dynamics simulations show that the autocorrelation function of the angular momentum usually displays a negative tail[1]; on the other hand, broad absorption band in the far infrared region[2] have been found. Both these observations are interpreted as a result of the librational motion of the molecules inside the cage potential instantaneously created by the surrounding molecules.

In this work we have investigated the structure and dynamical properties of the cage potential for a Gay-Berne mesogen in the isotropic and nematic phases. The methodology closely follows the analysis of cage effects in systems composed of linear molecules by Polimeno *et al.*[3].

THE MODEL SYSTEM

We have performed a molecular dynamics (MD) simulation for a system of 2000 molecules interacting via the Gay-Berne potential, GB(4.4,20.0,1,1). The first parameter represents the shape anisotropy of the ellipsoidal molecules, given by the ratio σ_e/σ_s, where σ_e and σ_s can be identified respectively with the length and the breadth of the repulsive core. The second coefficients gives the interaction anisotropy in terms of the ratio of the wells of the potentials for the side-by-side (ε_s) and the end-to-end (ε_e) configuration for a pair of molecules. The last parameters (usually labeled as ν and μ in the literature) are adimensional exponents without explicit physical meaning,

which can be chosen to adjust the details of the potential profiles. This model mesogen has been widely investigated by Bates and Luckhurst[4,5], who have determined the phase diagram using constant pressure Monte Carlo (MC) simulations. At a scaled pressure $P^* \equiv P\sigma_0^3/\varepsilon_0 = 2.0$, the system exhibits a nematic-isotropic transition at a scaled temperature $T_{NI}^* \equiv k_B T_{NI}/\varepsilon_0 = 1.675$; here, ε_0 and σ_0 are the scaling constants for the energy and the distance, respectively. The scaling factor ε_0 represents the attractive well depth of potential for a pair of molecules in the cross-configuration, and σ_0 is taken to be coincident with σ_s. For the analysis of the cage structure for this mesogen, we have selected two points in the phase diagram at $P^* = 2.0$, namely $T^* = 1.8$ (isotropic phase) and $T^* = 1.6$ (nematic phase) corresponding to a scaled number density $\rho^*_I \equiv \rho_I\sigma_0^3 = 0.1562$ and $\rho^*_N \equiv \rho_N\sigma_0^3 = 0.1756$, respectively.

The MD simulations were run in the microcanonical ensemble. The initial configurations were taken from the previous MC simulations[5] and were equilibrated for 25,000 timesteps. These equilibration runs were followed by production runs of 10,000 timesteps, during which time configurations were saved every 10 timesteps for later analysis. The timestep $\delta t^* \equiv \delta t(\varepsilon_0/m\sigma_0^2)^{1/2}$, where m is the mass of the particle, was set equal to 0.0025 and the moment of inertia $I_\perp^* \equiv I_\perp/m\sigma_0^2$ to unity, as in Ref. [5]. The simulations were run on the IBM SP2 at the University of Southampton and the analysis on the Cray T3E of the CINECA Consortium.

In order to test the applicability of the present study to real nematogens, we choose to describe the dynamical quantities such as time and frequency in ps and ps^{-1} respectively, rather than in scaled units, while the energy is expressed as U/k_BT. For the conversion of these quantities we have used the scaling parameters estimated in Refs. [4] and [5].

PARAMETERISATION OF THE CAGE POTENTIAL

Definition of the Cage

The theoretical definition of the cage potential is made according to the concepts introduced in Ref. [3]. It is worth noticing that the intuitive picture of the cage is given in term of the instantaneous potential confining the motion of each molecule for a fixed configuration of the surrounding particles and that we do not identify any particular shell of neighbouring molecules as representative of the cage. We start by defining the cage potential V_C as the interaction potential between the solute and the solvent molecules, calculated as a sum of the pair interactions of the test molecule with its neighbours up to a cutoff of $5.5\sigma_0$ (see Ref.[4]):

$$V_C = V(\underline{r}_O, \underline{\Omega}_O | \underline{X}), \tag{1}$$

where $\underline{r}_O$ represents the position of the centre of mass of the solute molecule, $\underline{\Omega}_O$ are the Euler angles defining the orientation of the molecular frame with respect to the laboratory frame and the parametric dependence from the configuration of the surrounding particles is indicated by the vector $\underline{X}$. Clearly, only the two polar angles α_O and β_O of $\underline{\Omega}_O$ need be defined to describe the orientation of a Gay-Berne molecule, due to its $D_{\infty h}$ symmetry.

In Fig. 1 we show two examples of cage potentials for the isotropic and nematic phase of the system investigated, as a function of the angle β_O between the molecular long axis and the Z laboratory axis; for the nematic phase, the Z axis corresponds to the director, while for the isotropic phase is taken arbitarily. We can see that the orientational phase space instantaneously accessible to the test molecule is very small, of the order of few degrees. The potential clearly has two equivalent minima for orientations differing by 180°, often it shows more than one minimum between $0° \leq \beta < 180°$, but the

barrier separating the various minima are always virtually infinite: because of the strong anisotropy in the shape of the mesogenic molecule it is impossible for it to rotate without overlapping substantially with other molecules. The cage potential represented in Fig. 1 is associated to a molecule chosen at random within the ensemble. By performing the analysis with a different test molecule the istantaneous profiles would be different but qualitatively similar. For comparison (see Fig. 1), we also report, for the nematic phase, a Maier-Saupe molecular field potential with a nematic barrier of 5.85 k_BT units such that the predicted order parameter is the same as that measured for our system at T* = 1.6, namely $\bar{P}_2$ = 0.70. It appears that the contribution of the mean field term is negligible with respect to the cage potential.

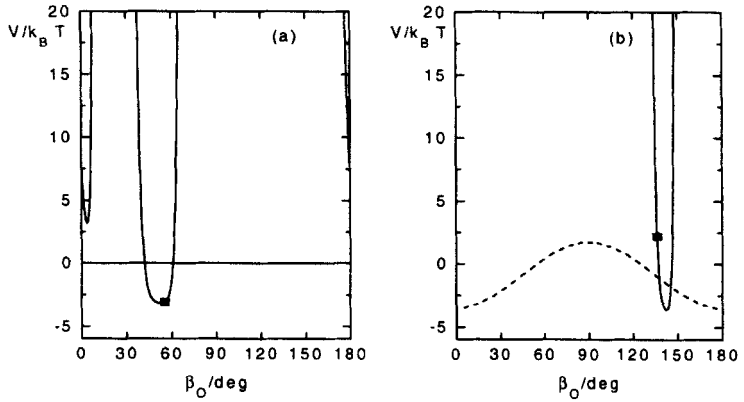

FIGURE 1: Cage potentials for a molecule chosen at random in (a) the isotropic and (b) the nematic phase. Squares represents the actual position of the molecule. For the nematic phase, a mean field potential (dash line), which predicts the orientational order parameter, $\bar{P}_2$, close to 0.70 (as measured in the nematic phase, see text) is reported for comparison.

Parameterisation of the Cage

In order to perform a statistical analysis of the cage we choose to expand the cage potential, up to second order, around its minimum. Eq. 1 is then reduced to:

$$V_C = V^{(0)}(r_C, \underline{\Omega}_C | \underline{X}) + V^{(2)}\left(\Delta \underline{r}_C, \Delta\underline{\Omega}_C, \underline{\underline{k}} | X\right), \qquad (2)$$

where $\underline{r}_C$ and $\underline{\Omega}_C$ represent the position and the orientation corresponding to the minimum of the potential, and will be identified, hereafter, as the position and orientation of the cage. In the second order term $\Delta\underline{r}_C$ and $\Delta\underline{\Omega}_C$ are the displacements from the equilibrium position and $\underline{\underline{k}}$ is the matrix of the gradients. Although significant anharmonic contributions to the cage potential are present, the harmonic approximation is the simpler form which accounts for the main features of the cage; the inclusion of higher terms of order n in the expansion requires the statistical evaluation of the corresponding tensor of rank n of the derivatives. Let us discuss, first of all, the zeroth order term $V^{(0)}$. For the isotropic phase the distribution of values of $V^{(0)}$ is independent of the cage coordinates $\underline{r}_C$ and $\underline{\Omega}_C$, due to the absence of orientational as well as long range translational order. In contrast, in the nematic phase, a significant dependence is observed on the polar angle β_C, (see Fig. 2(a)) defining the orientation of the cage z axis with respect to the director. The average value of each distribution $P(V^{(0)})$, is plotted versus the angle β_C in Fig. 2(b): its behaviour can be accurately described with a second order Legendre polynomial, with a barrier height of $\approx 2.0\ k_BT$. The distributions have been calculated after discretization of the angular coordinate β_C in sub-intervals $\Delta\beta_C = 10°$. In Fig. 2(a) the area is normalized to unity for both curves to facilitate the comparison.

We have calculated time dependent orientational correlation functions of the Legendre polynomial of first and second rank for the cage and, for comparison, for the molecule; they are reported in Fig. 3. We see that the orientational correlation function of the solute molecule and cage are nearly identical. This observation suggests, as already noted in Ref. [3], that we should interpret the diffusive dynamics of the molecule as a result of the diffusive motion of the cage. The molecule is constrained to follow its cage; however, librational degrees of freedom inside the cage remain. The ratio between the correlation times of first and second rank is very close to 3 for the isotropic phase (see Table 1), as expected for a diffusive motion; we also note the large slowing down of the first rank correlation function in the nematic phase, due to the presence of the nematic barrier.

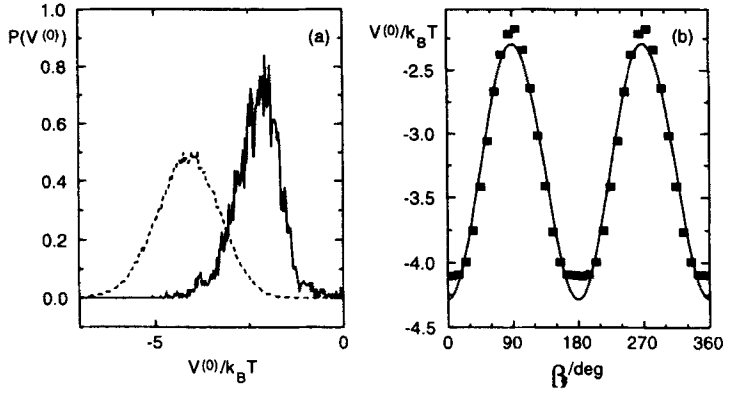

FIGURE 2: (a) Distribution of minima of the cage potential in the nematic phase, for perpendicular (solid) and parallel (dash) orientations of the cage z axis with respect to the director; (b) average value of several distributions vs the cage orientation.

In addition we report in Fig. 3 the correlation functions for the relative orientation of the molecule referred to the cage frame. The fast correlation time is related to the rapid fluctuations of the test molecule inside the cage. For the relative orientation we limit the analysis to the second rank correlation function, since the first rank is dominated by the dynamical process of barrier crossing between the two equivalent minima, differing by 180°, of the cage potential. Because of the large value of the barrier height (see Fig. 1) the correlation time of the first rank correlation function, of the relative orientation, tends to infinity.

TABLE 1: Correlation times of the observables discussed in the text

Isotropic phase	Nematic phase	
$\tau_O^1 = 36.4\,ps$	$\tau_O^1 = 1070\,ps$	molecule orientation[5]
$\tau_O^2 = 11.8\ ps$	$\tau_O^2 = 7.05\ ps$	molecule orientation[5]
$\tau_R^2 = 0.40\ ps$	$\tau_R^2 = 0.55\ ps$	relative orientation
$\tau_x^\omega = 0.52\ ps$	$\tau_x^\omega = 0.50\ ps$	librational frequency ω_x
$\tau_y^\omega = 0.52\ ps$	$\tau_y^\omega = 0.50\ ps$	librational frequency ω_y

The order parameter of the nematic phase is $\bar{P}_2 = 0.70$, where the overbar indicate an ensemble average. Using the properties of the Wigner functions we can write:

$$\bar{P}_2 = \overline{P_2(\cos\beta_O)} = \overline{D_{00}^2(\Omega_O)} = \overline{\sum_M D_{M0}^2(\Omega) D_{M0}^{2\,*}(\Omega_C)}, \tag{3}$$

where Ω is the relative orientation of the molecule with respect to the cage. The analysis of the MD data shows that the average on the left hand side of Eq. (3) can be factorised and that the molecular order parameter can be written as the product of the cage order parameter and the relative order parameter, namely the order parameter for the molecule with respect to the cage orientation: $\overline{P_2(\cos\beta_O)} = \overline{P_2(\cos\beta)} \cdot \overline{P_2(\cos\beta_C)}$ where $\overline{P_2(\cos\beta)}$=0.94 and $\overline{P_2(\cos\beta_C)}$=0.74. We finally remark that the order parameter for the relative orientation in the isotropic phase is roughly the same as for the nematic phase, namely $\overline{P_2(\cos\beta)}$=0.92. This indicate, as we will see more in detail in the next section, that the local structure of the two phases is only sligthly different.

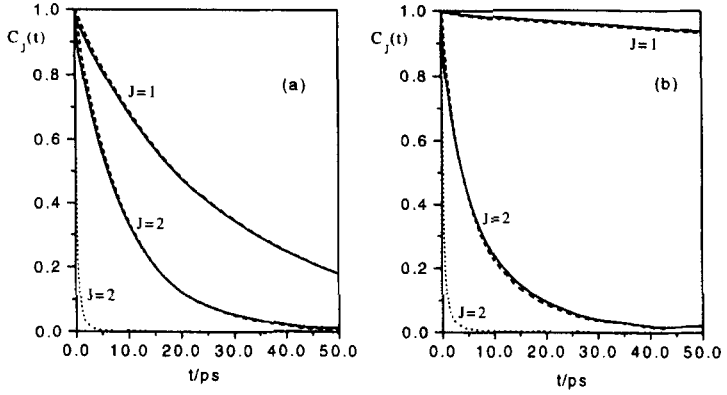

FIGURE 3: Orientational correlation functions of first (J=1) and second (J=2) rank in the isotropic phase (a) and nematic phase (b). Solid line: cage orientation; dash line: molecule orientation; dot line: relative orientation.

Analysis of the Curvatures

The second order term of Eq. 2 contains important information about the librational motion of the test molecules inside the cage potential, through the dependence on the curvature matrix. To reduce the complexity of the analysis we average out the translational coordinates assuming that they are much faster equilibrating than the orientational degrees of freedom. This assumption is not valid in general; nevertheless, the coupling terms between translation and rotation, in the curvature matrix, are about ten time smaller than diagonal elements. Following Ref. [3] we identify two independent librational frequencies, ω_x and ω_y, corresponding to the reorientational motion of the cage z axis.

In Table 2 we report the statistical values of the librational frequencies for both phases. We note that the two librational frequencies are equivalent and independent, since the average value of the product can be factorised. It seems that a significant difference exists between the isotropic and the nematic phase, but if we look at the distribution of ω_x and ω_y in Fig. 4(a) it is clear that the width of the distribution is much larger that the difference, in the average value, between the two phases. In fact, as noted before, the molecular field potential is nearly a constant with respect to the local potential felt by the test molecule. Such a result agrees with the results of MD simulations of this Gay-Berne system which show that, at short range, the second rank orientational correlation coefficient is very similar in the isotropic and nematic phase[4].

We have characterised also the time evolution of ω_x and ω_y, shown in Fig. 4(b). The trajectory shows very large fluctuations in time and can be conveniently interpreted as a result of the so-called "strong collision" regime in which the value of the coordinate at time t is independent of the value of the coordinate at the previous time t-δt. The strong collision model predicts a

decay with a characteristic time given by the inverse of the mean frequency of collision, which is weakly dependent upon temperature.

TABLE 2: Statistical properties of the librational frequencies

Phase	$\overline{\omega_x}$ / ps^{-1}	$\overline{\omega_y}$ / ps^{-1}	$\overline{\omega_x\omega_y}$ / ps^{-2}	$\overline{\omega_x^2}$ / ps^{-2}	$\overline{\omega_y^2}$ / ps^{-2}
I	2.32	2.32	5.39	6.85	6.85
N	2.62	2.61	6.89	8.68	8.68

Finally, in Fig. 5 we report the correlation functions of ω_x and ω_y. Again, it is clear that no differences appear in the decay times, reported in Table 1. It is interesting to note that the time window of the decay of the angular momentum correlation function is the same as that for the autocorrelation of ω_x and ω_y. In fact, the decay time of ω_x or ω_y can be interpreted as the "lifetime" of the cage. The comparison of the correlation times of the librational frequencies with the correlation times of the orientational motion indicate that a diffusive regime is rapidly reached for this system, as it also apparent from the rapid decay of the angular momentum correlation function.

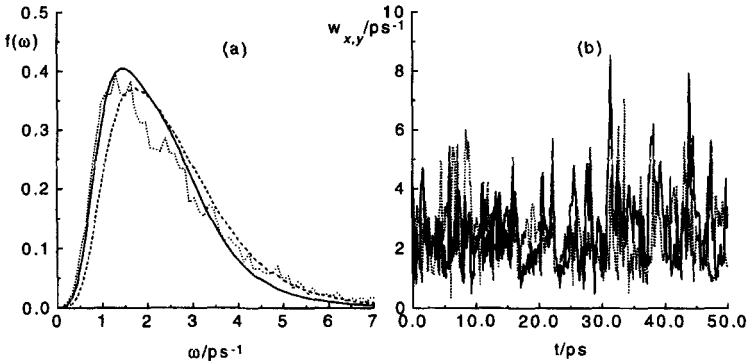

FIGURE 4: (a) Distribution of librational frequencies $\omega \equiv (\omega_x, \omega_y)$. Solid line: isotropic phase; dash line: nematic phase for the cage orientation perpendicular to the director; dot line: nematic phase for the cage parallel to the director. (b) trajectory of ω_x (solid) and ω_y (dot) for a molecule chosen at random

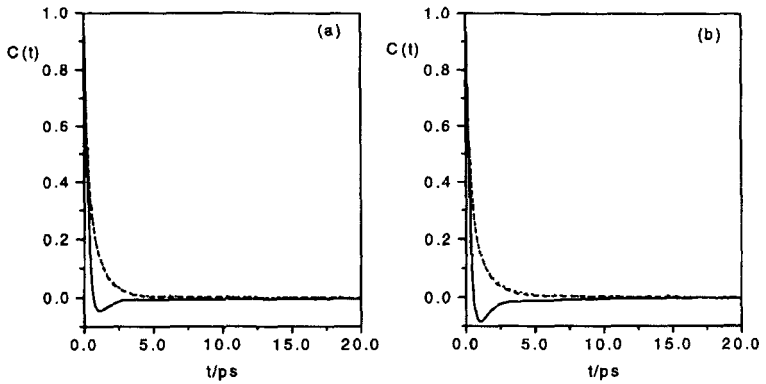

FIGURE 5: Correlation function for the angular momentum (solid), ω_x (dot) and ω_y (dash) in (a) the isotropic and (b) the nematic phase.

CONCLUSIONS

In this work we have characterised the structural and dynamical properties of the orientational cage for the Gay-Berne mesogen GB(4.4,20.0,1,1) in the isotropic and nematic phase. We have shown that the main difference between the two phases resides in the dependence of the distribution of the minima of the cage potential with respect to the cage orientation. Such a dependence is quite strong in the nematic phase and obviously absent in the isotropic phase. On the contrary, the distribution of the curvatures of the cage potential are nearly the same in the isotropic and nematic phases.

Acknowledgements

This work has been supported by the EC TMR contract FMRX-CT97-0121 and by the Italian Ministry for Universities and Scientific and Technological Research. We thank the CINECA Supercomputing Center in Bologna for the use of the parallel system CRAY T3E and the Southampton University Computer Services for generous acces to the IBM SP2. The authors would like to thank Mr. Diego Frezzato for his valuable collaboration and Prof. Giorgio J. Moro for enligthening discussions.

This paper is dedicated to the memory of Prof. Pier Luigi Nordio.

References

[1] D.J. Tildesley and P.A. Madden, *Mol. Phys.*, **48,** 129 (1983).
[2] A. Gershel, in *Molecular Liquids,*edited by A. Barnes, W. Orville-Thomas and J. Yarwood (Reidel, Boston, 1984), NATO Advanced Study Institutes, Ser. C, vol. 135, p.163.
[3] A. Polimeno, G.J. Moro and J.H. Freed, *J. Chem. Phys.*, **102,** 8094 (1995).
[4] M.A. Bates and G.R. Luckhurst, *J. Chem. Phys.*, in submission..
[5] M.A. Bates, PhD thesis, Southampton 1996.